A&A 465, 899–906 (2007)
DOI: 10.1051/0004-6361:20065278

Astronomy & Astrophysics

Linear and circular polarisation of diffuse interstellar bands⋆

N. L. J. Cox[1,⋆⋆], N. Boudin[2], B. H. Foing[2], R. S. Schnerr[1], L. Kaper[1], C. Neiner[3], H. Henrichs[1], J.-F. Donati[4], and P. Ehrenfreund[5]

[1] Astronomical Institute "Anton Pannekoek", Universiteit van Amsterdam, Kruislaan 403, 1098-SJ Amsterdam, The Netherlands
e-mail: Nick.Cox@esa.int
[2] ESA Research and Scientific Support Department, PO Box 299, 2200-AG Noordwijk, The Netherlands
[3] GEPI, UMR 8111 du CNRS, Observatoire de Paris-Meudon, 5 place Jules Janssen, 92195 Meudon Cedex, France
[4] Laboratoire d'Astrophysique de l'Observatoire Midi-Pyrénées, 14 avenue Edouard Belin, 31400 Toulouse, France
[5] Astrobiology group, Leiden Institute of Chemistry, Leiden University, Einsteinweg 55, 2300-RA Leiden, The Netherlands

Received 27 March 2006 / Accepted 19 January 2007

ABSTRACT

Context. The detection or absence of a polarisation signal in the diffuse interstellar band (DIB) profile can possibly give important clues on the identity of its carrier. For molecular gas-phase carriers the effect of polarisation on its electronic transitions depends, although uncertain how exactly, on its physical properties (e.g. molecular structure). On the other hand, if the carriers are grains, impurities or defects in grain mantles are also expected to show up in the polarisation of DIBs.
Aims. Our aim is to detect a polarisation signal in a DIB profile or to derive stricter upper limits on the polarisation efficiency of DIB carriers.
Methods. In order to detect and measure the linear and circular polarisation of the DIBs we observe reddened lines of sight showing continuum polarisation; for this study we select the stars HD 21219, HD 198478, HD 197770, HD 183143 and HD 163472. We use spectropolarimetry in the wavelength range 4480 to 6620 Å with the MuSiCoS échelle spectrograph mounted at the Télescope Bernard Lyot.
Results. Linear polarisation spectra are constructed in order to search for a polarisation signal in the DIB profiles. No significant change in the linear polarisation degree is found. We obtain a 2σ polarisation detection limit (per DIB *FWHM*) of 0.01−0.04% for HD 21219, 0.04−0.14% for HD 197770, 0.01−0.14% for HD 183143 and 0.01−0.14% for HD 198478, for the six investigated DIBs. We derive upper limits for the polarisation efficiency factor f for six strong narrow DIBs; $f_{\max}$ of 0.31, 0.44, 0.45, 0.18, 0.47 and 0.68 for the $\lambda\lambda$ 5780, 5797, 6196, 6284, 6379 and 6613 DIBs, respectively. The derived detection limits are similar to those derived by Adamson & Whittet (1995), although for more lines of sight and more DIBs. Circular polarisation (Stokes V) spectra of high signal-to-noise have been obtained for the first time for the 5780, 5797, 6196, 6203, 6284, 6376, 6379 and 6613 Å DIB profiles. No circular polarisation signal is detected. The $2\sigma_V$ (per 0.1 Å) noise level limits are 1.0−2.5% for the DIBs in the line of sight towards HD 197770 and 0.06−0.10% for the DIBs towards HD 163472.
Conclusions. The lack of polarisation of the DIB profiles is consistent with DIB carriers that are not directly related to solid features, like impurities in grain mantles. However, large (carbonaceous) gas phase molecules remain viable DIB carrier candidates.

Key words. astrochemistry – polarisation – ISM: dust, extinction – ISM: lines and bands – ISM: molecules

1. Introduction

The diffuse interstellar bands (DIBs) are absorption bands seen – from the blue to the near-infrared light – in the spectra of stars obscured by one or several interstellar clouds. The DIBs were first reported by Heger (1922) and their interstellar nature was firmly established by Merrill (1934). Today, more than 300 DIBs – differing in strength, shape and/or width – are indexed, but the identity of the carriers remains a longstanding mystery. Observational properties of the DIBs constrain their origin in the interstellar medium (Merrill 1934; Herbig 1995). DIBs are observed throughout the Galaxy (Herbig 1993), the Magellanic Clouds (Ehrenfreund et al. 2002; Cox et al. 2006, 2007; Welty et al. 2006), and beyond (Heckman & Lehnert 2000; Sollerman et al. 2005). Several DIBs respond to the local environmental conditions, in particular to the effective strength of the UV field (e.g. Cami et al. 1997). Their strength variation could reflect the local charge state balance of the carrier molecules (Ruiterkamp et al. 2005; Cox & Spaans 2006). The identified substructure in DIB profiles is indicative of large (complex carbonaceous) gas phase molecules (Sarre et al. 1995; Ehrenfreund & Foing 1996). Therefore, specific groups of stable UV resistant molecules (such as PAHs, fullerenes and carbon chains) are commonly postulated carrier candidates (Leger & D'Hendecourt 1985; Crawford et al. 1985).

The presence or absence of a polarisation signal in the DIB profile could show a relation between proposed DIB carriers and the type of grains responsible for the linear or circular continuum polarisation of stellar light passing through the interstellar medium. However, no theoretical predictions are available to predict the polarisation signal (neither qualitatively nor quantitatively) from PAHs and fullerenes in the interstellar gas phase (see also the discussion; Sect. 4).

⋆ Based on observation at the Observatoir du Pic du Midi, France with the MuSiCoS spectropolarimeter.

⋆⋆ *Present address*: European Space Astronomy Centre, Research and Scientific Support Department of ESA, Villafranca del Castillo, Apartado de Correos 50727, 28080 Madrid, Spain.

The overall polarisation related to interstellar extinction is due to the alignment (e.g. by the Galactic magnetic field) of non-spherical grains along the line of sight. The presence of DIB carriers on the grain surface (or embedded in the grain) could perhaps give rise to a small change Δp in polarisation p, proportional to the optical depth change, across the profile (Greenberg & Hong 1974; Martin & Angel 1974; Somerville 1996):

$$\Delta p \sim f\ p\Delta\tau/\tau, \quad (1)$$

where τ and p are the continuum optical depth and the continuum polarisation, respectively; $\Delta\tau$ is the observed increase/decrease in optical depth across the DIB feature, and f is the polarisation efficiency factor. Martin & Angel (1974) found f to be between 1.0 and 1.8 for classical grains, covering a range in composition and morphology. For perfectly aligned grains $\Delta p/\Delta\tau_{\rm pa} \sim 0.8$ (Martin et al. 1995).

There have been several attempts to measure linear polarisation of the DIBs (Gammelgaard & Rudkjobing 1973; Martin & Angel 1974, 1975; Fahlman & Walker 1975; Adamson & Whittet 1992, 1995). These studies concentrated on the broad DIB at 4430 Å and the three strong narrow DIBs $\lambda\lambda$ 5780, 5797, 6284 (Table 1). No linear polarisation of DIBs has been detected. Lines of sight with a high linear continuum polarisation ($p > 3.0\%$) and a high reddening ($E_{(B-V)} > 0.55$ mag) exhibit also a small circular continuum polarisation of ~0.005% (e.g. Michalsky et al. 1974; Avery et al. 1975). As of yet, no attempt has been made to search for circular polarisation of DIBs, although there are several mechanisms that could give rise to it (see also the discussion; Sect. 4).

We report for the first time high-resolution, high signal-to-noise spectropolarimetric spectra in order to search for linear and circular polarisation in DIB profiles between 4480 and 6620 Å. First we describe the acquired spectropolarimetric observations of linear polarisation of six DIBs towards four targets and circular polarisation of seven DIBs towards two targets (Sect. 2). The polarisation P spectra, derived from the Stokes Q and U spectra, are discussed in Sect. 3, together with the predicted classical grain line polarisation profile. Subsequently, linear and circular Polarisation Detection Limits PDL (%), and upper limits on the linear polarisation efficiency factor f, are presented. The results and their implications for the identification of the DIB carriers are discussed in Sect. 4.

2. Observations

We selected previously studied lines of sight towards early-type stars that are known to show a high continuum polarisation, and are significantly extincted by dust (i.e. have a high reddening). The characteristics of the selected targets/sightlines and the journal of the spectropolarimetric observations are summarised in Tables 1 and 2. The linear polarisation observations were obtained during two runs, in October 2003 and June 2004, with the fibre-fed MuSiCoS cross-dispersed échelle spectropolarimeter mounted at the f/25 Cassegrain focus of the 2-m Télescope Bernard Lyot (TBL) at Pic du Midi in France. The instrumental polarisation is small (less than 10^{-4}), which allows the recording of interstellar polarisation in the visible range from 4480 to 6620 Å, with a spectral resolution of 35 000 (Donati et al. 1997, 1999). The optical characteristics of the polarisation analyser, as well as the spectropolarimeter observing procedures, are described in detail by Donati et al. (1999).

For each target and each Stokes parameter (Q, U or V) we obtained sequences of four sub-exposures between which either the instrument or the $\lambda/4$-retarder is rotated by ±90°. This procedure should ensure the suppression of all first-order spurious polarisation signatures down to a level of 10^{-4} (Donati et al. 1997). For the linear polarisation exposures we achieved signal-to-noise levels up to 1500 at 5800 Å for the total intensity spectra (see Table 2). About 140 circular polarisation Stokes V spectra of V2052 Oph were obtained previously (between 2000 and 2003) by three of us (RS, CN and HH) to search for stellar surface magnetic fields (Neiner 2002). The averaged total intensity spectrum of V2052 Oph has a continuum signal-to-noise of about 2000−2500, except for the edge of the spectral range where it drops to about 1400.

The sub-exposures are combined during the reduction procedure to generate the transmittance spectra and the respective Stokes parameter spectrum. The data reduction was performed with the ESPRIT reduction package (Donati et al. 1997). The geometry of the orders on the CCD was first determined. Then, after an automatic wavelength calibration on the ThAr frames a rigorous optimal extraction of the orders was performed. The total intensity spectra are normalised to unity during the data processing, and the Stokes Q/I, U/I and V/I parameter spectra can thus be directly read as the degree of linear (Q or U) or circular (V) polarisation. Multiple spectra obtained for each Stokes parameter and each line of sight were averaged, with weights determined per pixel from the intensity error which is derived during the reduction process.

Table 1. Summary of previously reported observations on the polarisation of DIBs. The spectral type, visual magnitude V, reddening $E_{(B-V)}$, continuum polarisation for each target are given in Cols. (2) to (5), respectively. The DIB polarisation detection limit DL is given in (Col. 6). For each line of sight the previously observed DIBs and references are given in Cols. (7) and (8).

Target	Spectral type	V (mag)	$E_{(B-V)}$ (mag)	p (%)	DL (%)	DIBs (λ)	Ref
HD 183143	B7Ia	6.917	1.28	5.886	–	4430	1
					–	4430 & 5780	2
					0.4	6284	3
					0.5	5797	4
HD 197770	B2III	6.341	0.58	4.150	0.03	5797, 5778	4
						& 5780	4
HD 13854	B1Iabe	6.499	0.47	3.730	–	4430	1
HD 21291	B9Ia	4.259	0.43	3.395	–	4430	1
HD 21389	A0Iab	4.60	0.55	3.280	–	4430	1
					0.5	4430 & 6284	5
HD 194279	B1.5Ia	7.09	1.20	2.900	0.5	5797	4
HD 198478	B3Iae	4.858	0.54	2.877	–	4430	1

[1] A'Hearn (1972); [2] Martin & Angel (1974); [3] Fahlman & Walker (1975); [4] Adamson & Whittet (1995) ($S/N \sim 1000$ per 0.8 Å); [5] Martin & Angel (1975).

3. Polarisation across DIB profiles

We have observed the spectral range from 4480 to 6620 Å, which covers many DIBs. DIBs are generally weak spectral features, thus we focus on the strongest bands available in the observed spectral range. We select those DIBs that generally have a central depth greater than 7% (e.g. Jenniskens & Désert 1994; Herbig 1995; Tuairisg et al. 2000): $\lambda\lambda$ 5780, 5797, 6196, 6284, 6379 and 6613. For each target the selected DIB equivalent widths per unit reddening are measured in the total intensity spectra (Table 3).

Table 2. Summary of the new spectropolarimetry observations obtained with TBL/MuSiCoS. HD 163472 or V2052 Oph (B2IV/V = 5.834 mag, $(B-V) = 0.05$ mag, $E_{(B-V)} \sim 0.29$ mag) and HD 174638 or * bet Lyr A (B7Ve, $V = 3.52$ mag, $(B-V) = 0.00$ mag, $E_{(B-V)} \sim 0.135$ mag) are the two reddened lines of sight not previously studied in this context. All spectra cover the wavelength range from 4480 to 6620 Å. $\tau_V/p_{\max}$ gives the ratio of the continuum optical depth over the continuum polarisation; see Eq. (2). For optimal alignment the maximum polarisation efficiency is $p_{\max}/\tau_V \sim 0.032$ or $\tau_V/p_{\max} \sim 31.25$ (Serkowski et al. 1975). $S/N_{\rm I}$ is the signal-to-noise of the total transmittance spectrum at about 5800 Å. [(1)] PDLP is the 1σ Polarisation Detection Limit per Pixel (1 pixel = 0.06 Å), measured across 1 Å at 5800 Å. [(2)] PDLA is the 1σ Polarisation Detection Limit per 0.8 Å (≈16 pixels), which is equal to the resolution obtained by Adamson & Whittet (1995).

Targets Reddened:	$E_{(B-V)}$ (mag)	A_V (mag)	$\tau_V/p_{\max}$	Stokes	Date of observation	Exp. (min)	$S/N_{\rm I}$	PDLP[(1)] (%)	PDLA[(2)] (%)
HD 183143	1.28	3.72[1]	58.2	U, Q	October 2004	360	270	0.4	0.12
					June 2004	540	400	~0.2	
HD 197770	0.58	1.61 ± 0.14[2]	35.7	U, Q	October 2003	360	528	0.2	0.08
					June 2004	120	260		
				V	October 2003	60	305	0.9	0.3–0.7
HD 21291	0.43	1.48[1]	41.5	U, Q	October 2003	360	1487	0.06	0.04
HD 198478	0.54	1.48 ± 0.19[2]	47.4	U, Q	June 2004	520	1160	0.08	0.05
HD 163472	0.29	0.9[3]		V	June/July 2000, 2001, 2002	1242	2000	~0.1	0.04
HD 174638	0.135	0.4[3]	46.0	U, Q	June 2004	312	1500		
Standard:									
HD 109387	0.04			U, Q	June 2004	232	1500		

References: [1] Ducati et al. (2003); [2] Valencic et al. (2004); [3] average ISM value adopted: $R_V = 3.1$.

Table 3. DIB equivalent width per unit reddening (EW/$E_{(B-V)}$ in mÅ) for the reddened targets, with typical errors of less than 10%.

	DIB equivalent width per unit reddening (mÅ)				
$\lambda_{\rm DIB}$ (Å)	HD 183143	HD 197770	HD 198478	HD 21291	HD 163472
$E_{(B-V)}$ (mag)	1.28	0.58	0.54	0.43	0.29
5780.55	590	253	581	460	741
5797.08	164	148	146	165	266
6195.99	64	43	63	47	86
6379.22	91	107	152	74	245
6613.63	288	197	226	193	410

Any polarisation signal within a DIB profile is spread over the entire width of the feature, thus favouring the narrow lines. Note that it is not necessary at all that the strong narrow DIB carriers are also the most efficient polarisers, nor the most abundant. The carriers of the weak DIBs could very well produce significantly more polarisation, and have higher *S/N*. However, we have no a priori information on the polarisability efficiencies of the DIB carriers, which would scale with the amount of material (i.e. column density/optical depth). For example, a weak DIB could be a result of a small oscillator strength of the particular electronic transition, while the polarisability could be large relative to the line strength. Therefore, we look at the strong narrow DIBs that show the largest maximum optical line depth. In this way, because a larger optical depth requires a less stringent detection limit to exclude the grain model, we can in effect achieve stricter upper limits for f.

The Stokes Q and U spectra are combined to give the polarisation spectrum $P = \sqrt{Q^2 + U^2}$. A search for a polarisation signature revealed no polarisation signal across any of the selected strong DIBs (Figs. 1 to 4). The theoretical change in polarisation across the DIB profile is given by Eq. (1), which can be re-written as

$$f = \frac{\Delta p}{\Delta \tau} \frac{\tau}{p} \tag{2}$$

with τ and p determined by the observed extinction A_V and continuum polarisation (Tables 1 and 2); Δp and $\Delta \tau$ are measured from the spectra. The polarisation efficiency is defined as $\eta = \Delta p/\Delta \tau = f\ p/\tau$. The continuum optical depth is given by $A_\lambda = -2.5 \log (I_\lambda/I_0) = 1.086 \tau_{\rm continuum,\lambda}$. The observed intensity profile is converted to an optical depth profile: $\Delta \tau_{\rm line} = \ln (I_{\rm c}/I_\lambda)$. Together with the continuum polarisation p this gives an expected polarisation profile Δp, fixed by one free parameter, f.

First we compute, for each DIB in all lines of sight, the predicted profile expected for the classical grain scenario for which f lies between 1.0 and 1.8 for a variety of grain geometries and compositions (Martin & Angel 1974, 1975). Figures 1 to 4 show the resulting polarisation profiles (green) overplotted on the observed polarisation spectra. Note that the 6284 Å DIB Stokes I (i.e. total intensity) spectra needed to be corrected for the telluric oxygen bandhead. This is done by dividing the observed intensity spectrum by that of a non-reddened standard star (HD 109387), scaled to match the telluric lines in central depth, thus cancelling out the telluric lines.

The achieved statistical noise level of the polarisation spectrum, σ_P, determines the polarisation detection limit, and thus an upper limit for f (Table 5). Taking $2\sigma_P$ as the limit for the polarisation change Δp directly yields the corresponding maximum absolute value for f, $f_{\max}$ (Eq. (2)). The corresponding polarisation profiles for $f_{\max}$ are plotted in Figs. 1 to 4. We also computed the 2σ Polarisation Detection Limit per $FWHM_{\rm DIB}$, *PDLF* (%), which is derived from the statistical 2σ noise per pixel (i.e. 0.05 Å), by dividing by $\sqrt{n}$, with n the number of pixels per $FWHM_{\rm DIB}$. Similarly, we compute the 2σ Polarisation Detection Limit per Å (*PDLA*). Table 5 lists the *PDLF* (%) and the *PDLA* (%) for the linear polarisation of the six narrow DIBs investigated towards the four reddened targets. These values are also shown in the respective panels of Figs. 1 to 4.

Figure 5 shows the Stokes I (total intensity) DIB spectrum towards HD 163472 together with the observed Stokes V/I spectrum plotted on top, with a vertical offset of 1.025, and vertically expanded by a factor 10, for clarity. Figure 6 shows the total intensity Stokes I and the circular polarisation Stokes V/I, offset by 1.025, for HD 197770. For the circular polarisation we derive $2\sigma_V$ instrumental noise levels (Table 4) and use these as the detection limit.

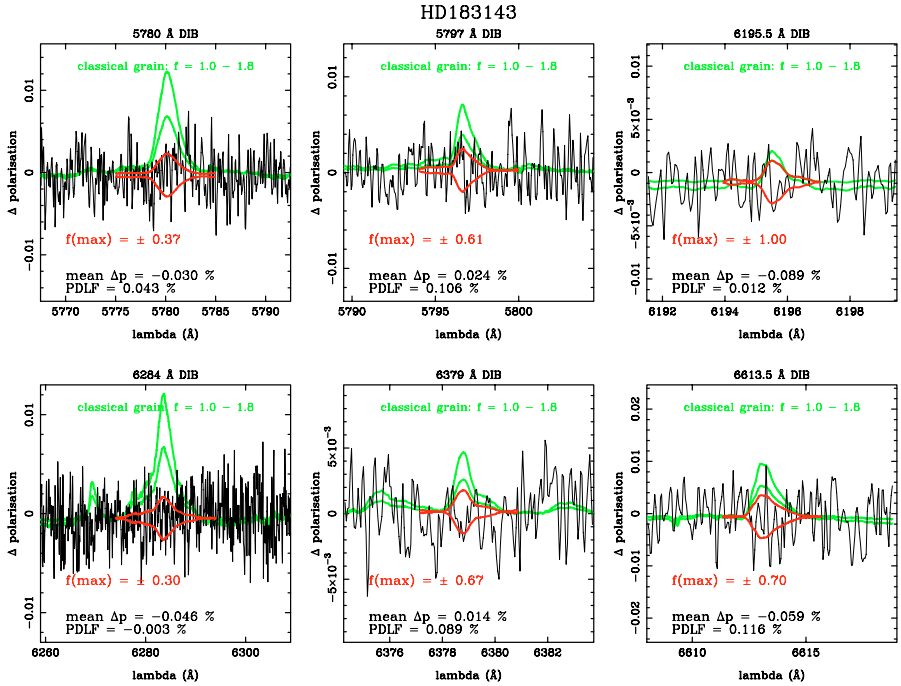

Fig. 1. Linear polarisation: ΔP for the $\lambda\lambda$ 5780, 5797, 6196, 6284, 6379 and 6613 DIBs towards HD 183143. The polarisation change predicted for grain related carriers is indicated by the solid green lines for $f = 1.0$ and $f = 1.8$, respectively The maximum absolute value for f, $f_{\rm max}$, the mean polarisation change, $\Delta\bar{p}$ (%), and the Polarisation Detection Limit per *FWHM*, PDLF (%), are indicated in each panel. $f_{\rm max}$ is computed from Eq. (2) using the observed maximum optical line depth, $\tau_{\rm line,\ max}$ for the DIB, the 2σ noise level in the polarisation spectrum, $2\sigma_P$, together with the known values for the continuum optical depth and the continuum polarisation. The predicted polarisation changes for $\pm f_{\rm max}$ are shown as red curves. See Sect. 3 for more details. Note the different wavelength scale for each panel.

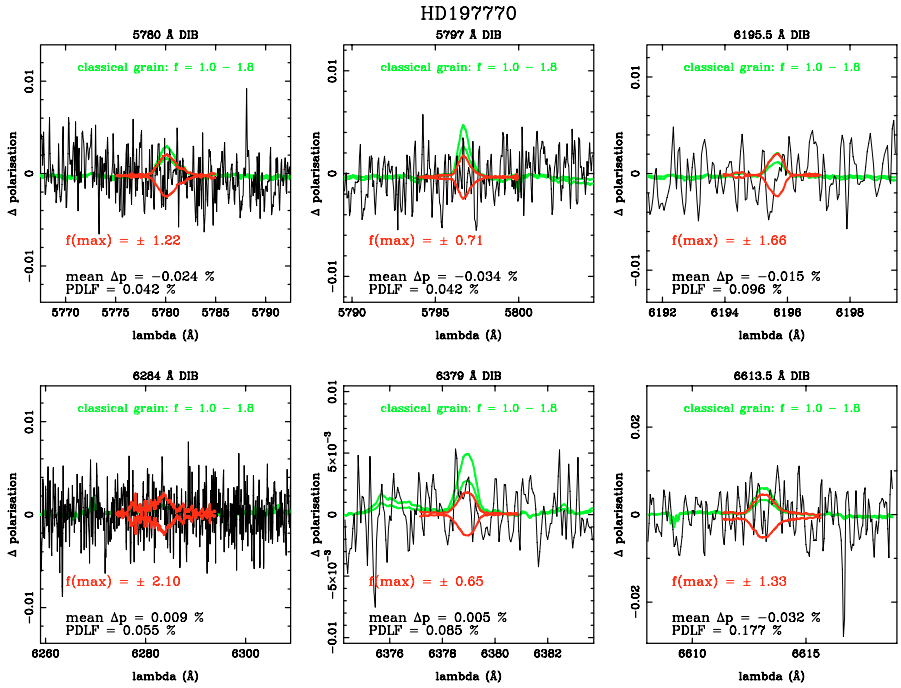

Fig. 2. Linear polarisation: ΔP for the $\lambda\lambda$ 5780, 5797, 6196, 6284, 6379 and 6613 DIBs towards HD 197770 In each panel we quote $f_{\rm max}$ and $\Delta\bar{p}$ (%) and the PDLF (%) (see also Fig. 1).

4. Discussion

Despite the non-detection of linear and circular polarisation reported above, this study is encouraging because it provides a new systematic approach for studying the polarisation signature of DIBs. With the availability of échelle spectropolarimeters it is now possible to study a well defined sample of sight lines over a large wavelength range. This allows us to perform a systematic search for linear and circular polarisation of many DIBs (in stark contrast to the limited number of DIBs studied in the past) in lines of sight probing different environmental conditions. This is the first time that the six strongest DIBs in the range 4480

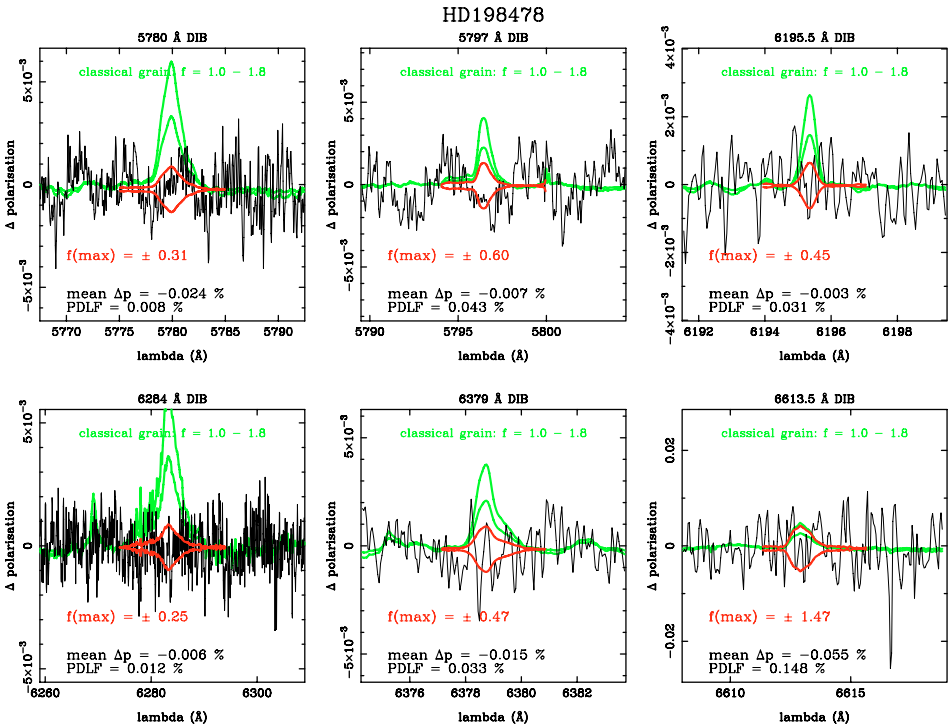

Fig. 3. Linear polarisation: $\Delta\bar{p}$ for the $\lambda\lambda$ 5780, 5797, 6196, 6284, 6379 and 6613 DIBs towards HD 198478. In each panel we quote $f_{\rm max}$ and $\Delta\bar{p}$ (%) and the PDLF (%) (see also Fig. 1).

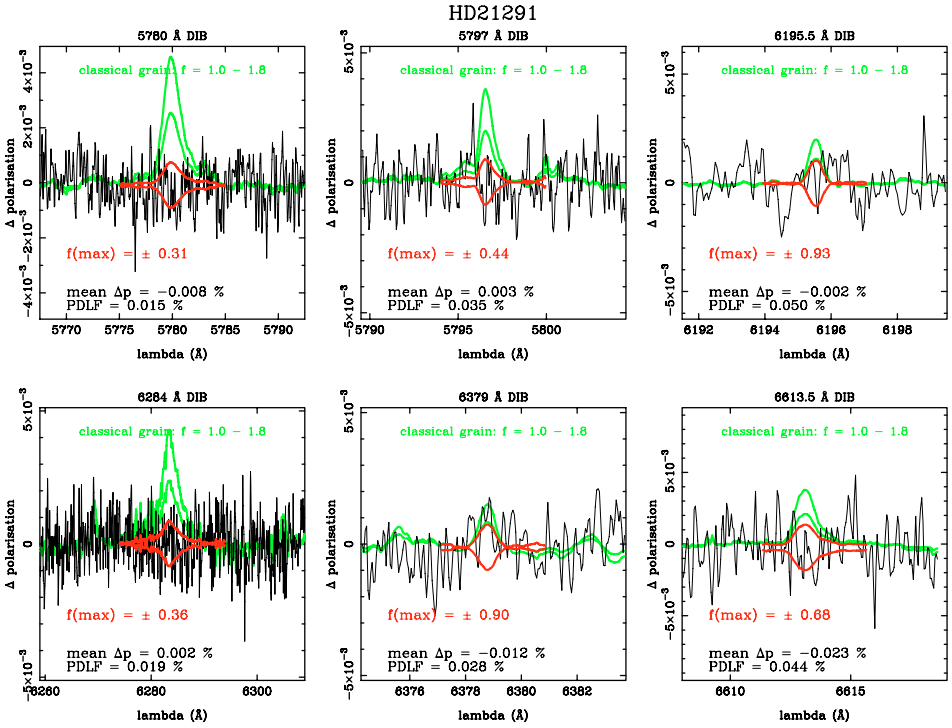

Fig. 4. Linear polarisation: ΔP for the $\lambda\lambda$ 5780, 5797, 6196, 6284, 6379 and 6613 DIBs towards HD 21291. In each panel we quote $f_{\rm max}$ and $\Delta\bar{p}$ (%) and the PDLF (%) (see also Fig. 1).

to 6620 Å have been investigated for linear (4 sightlines) and circular (2 sightlines) polarisation features. No polarisation signal could be detected in any DIB profile.

We report instrumental noise polarisation detection limits (*PDLF*) between 0.01 and 0.14%, an order of magnitude lower than previously obtained for most lines of sight. The most stringent detection limits, *PDLF* $\sim$ 0.01%, are found for the 6284 Å DIB. A polarisation detection limit of 0.03% per 0.8 Å was previously achieved by Adamson & Whittet (1995), but only for the $\lambda\lambda$ 5797, 5778 and 5780 DIBs towards HD 197770. In comparison, we obtained *PDLA* 0.08 and 0.06% for the 5780 and 5797 Å DIBs in this line of sight, respectively. In addition, we find a range of maximum values for the polarisation efficiency factor, $f_{\rm max}$ are 0.31, 0.44, 0.45, 0.18, 0.47 and 0.68,

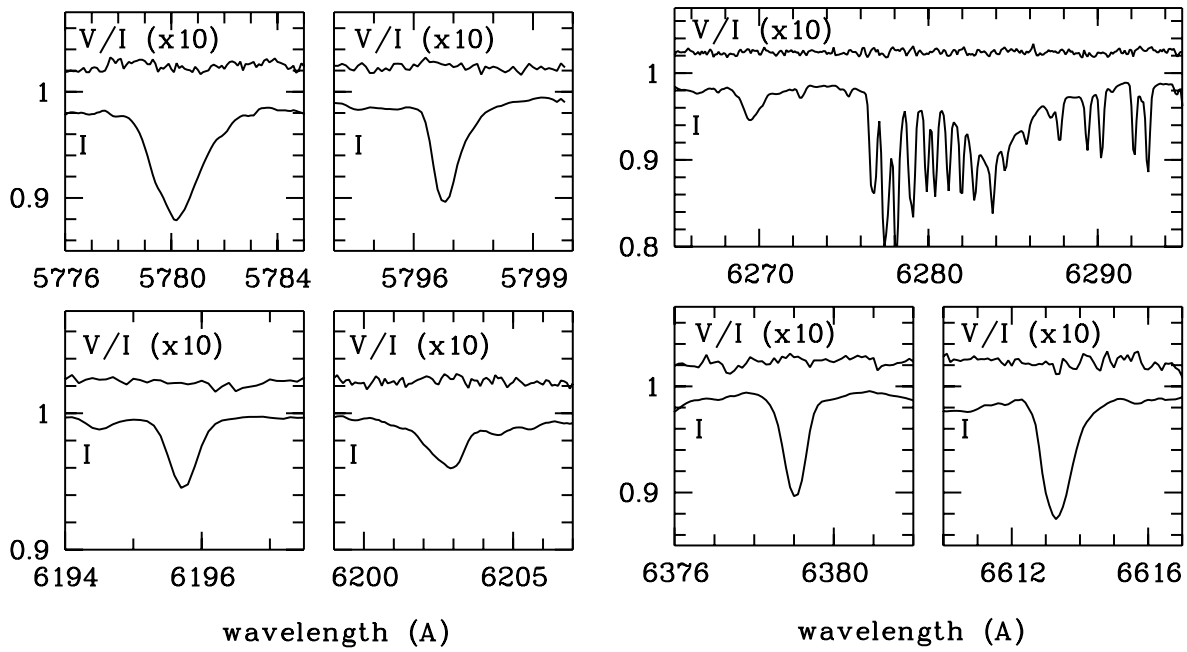

Fig. 5. Circular polarisation: Stokes parameters I and V/I (multiplied by 10) for the 5780, 5797, 6196, 6203, 6284, 6379 and 6613 Å DIBs towards HD 163472. $2\sigma_V$ (per pixel) polarisation noise detection limits are given in Table 4. No significant contamination of stellar lines (for early-type stars) is expected for the DIBs shown above. The B2 IV/V (T = 20 000 K) synthetic spectrum by Gummersbach & Kaufer (1996) shows a 3.6 mÅ Fe II line at 5780.13 Å and a 7.5 mÅ N II at 6379.617 Å. A few S II lines are present in the red wing of the 6284 Å DIB (1.5 mÅ at 6286.34, 17.2 mÅ at 6286.94 and 1.0 mÅ at 6289.44 Å). Several other weak stellar lines in the plotted ranges fall outside the DIB profiles. Note that the atmospheric water lines (the sharp features in the 6284 Å DIB panel) are not polarised.

Table 4. DIB Polarisation Detection Limit (%) per *FWHM* Å (PDLF) and per Å (PDLA). For the circular polarisation (Stokes V) the $2\sigma_V$ instrumental noise per pixel (0.1 Å) is taken as the detection limit.

		HD 183143		HD 197770		HD 198478		HD 21291		HD 163472	HD 197770
	$E_{(B-V)}$	1.28		0.58		0.54		0.43		0.29	0.58
$\lambda_{\rm DIB}$ (Å)	*FWHM* (Å)	PDLF (%)	PDLA (%)	PDLF (%)	PDLA (%)	PDLF (%)	PDLA (%)	PDLF (%)	PDLA (%)	$2\sigma_V$ (%)	$2\sigma_V$ (%)
5780.55	2.5	0.10	0.09	0.04	0.08	0.04	0.03	0.01	0.03	0.08	1.1
5797.08	1.5	0.13	0.12	0.04	0.06	0.06	0.05	0.03	0.04	0.07	1.8
6195.99	0.8	0.12	0.00	0.07	0.08	0.09	0.03	0.04	0.04	0.06	1.5
6284.09	5.0	0.01	0.05	0.06	0.11	0.01	0.04	0.01	0.04	0.06	1.0
6379.22	0.95	0.10	0.09	0.08	0.08	0.08	0.03	0.04	0.03	0.06	1.5
6613.63	1.1	0.14	0.13	0.14	0.19	0.14	0.16	0.04	0.05	0.10	2.5

Table 5. DIB polarisation 2σ upper limit $f_{\rm max}$, the maximum of the polarisation efficiency factor f.

		HD 183143	HD 197770	HD 198478	HD 21291
$\lambda_{\rm DIB}$ (Å)	*FWHM* (Å)	$f_{\rm max}$	$f_{\rm max}$	$f_{\rm max}$	$f_{\rm max}$
5780.55	2.5	0.37	1.22	0.31	0.31
5797.08	1.5	0.61	0.71	0.60	0.44
6195.99	0.8	1.00	1.66	0.45	0.93
6284.09	5.0	0.28	0.40	0.18	0.19
6379.22	0.95	0.68	0.66	0.47	0.87
6613.63	1.1	0.69	1.36	1.49	0.68

for the $\lambda\lambda$ 5780, 5797, 6196, 6284, 6379 and 6613 DIBs, respectively. The previously reported upper limit on f, $f_{\rm max}$ is 0.56 for the 5780 Å DIB (Martin & Angel 1974), $f = -0.13 \pm 0.11$ (i.e. $f_{\rm max} = 0.09$), and 0.044 ± 0.14 (i.e. $f_{\rm max} = 0.32$) for the 5780 and 5797 Å DIBs towards HD 197770, respectively (Adamson & Whittet 1995). These values exclude classical grains as carriers of the $\lambda\lambda$ 5780, 5797, 6613 and 6284 DIBs. That the 6379 and 6613 Å DIBs originate from (classical) grains can only be marginally excluded.

The lack of line polarisation of DIBs implies that the DIB carriers are not embedded in or stuck onto large grains (i.e. those that produce optical extinction and polarisation), but might still be related to smaller grains, i.e. those that produce the far-UV extinction, or large gas phase molecules. However, the lack of correlation between DIB strengths and the far-UV extinction also seems to exclude a common carrier. Hence, the lack of polarisation seems to indicate that the carriers (of those DIBs studied) are in the gas phase. This idea is consistent with the observed substructure in the profile of some DIBs reminiscent of rotational contours of free molecules (Sarre et al. 1995; Ehrenfreund & Foing 1996; Kerr et al. 1996; Cami et al. 2004).

The lack of polarisation (polarisation efficiency $\eta = \Delta p/\Delta\tau < 0.2$) of the 3.4 μm absorber (e.g. hydrogenated amorphous carbon) in the diffuse medium is well below that expected for a carrier associated with impurities in the mantles of aligned grains (Pendleton et al. 1994; Sandford et al. 1991; Chiar et al. 2006). The UV 2175 Å bump is devoid in polarisation, with the

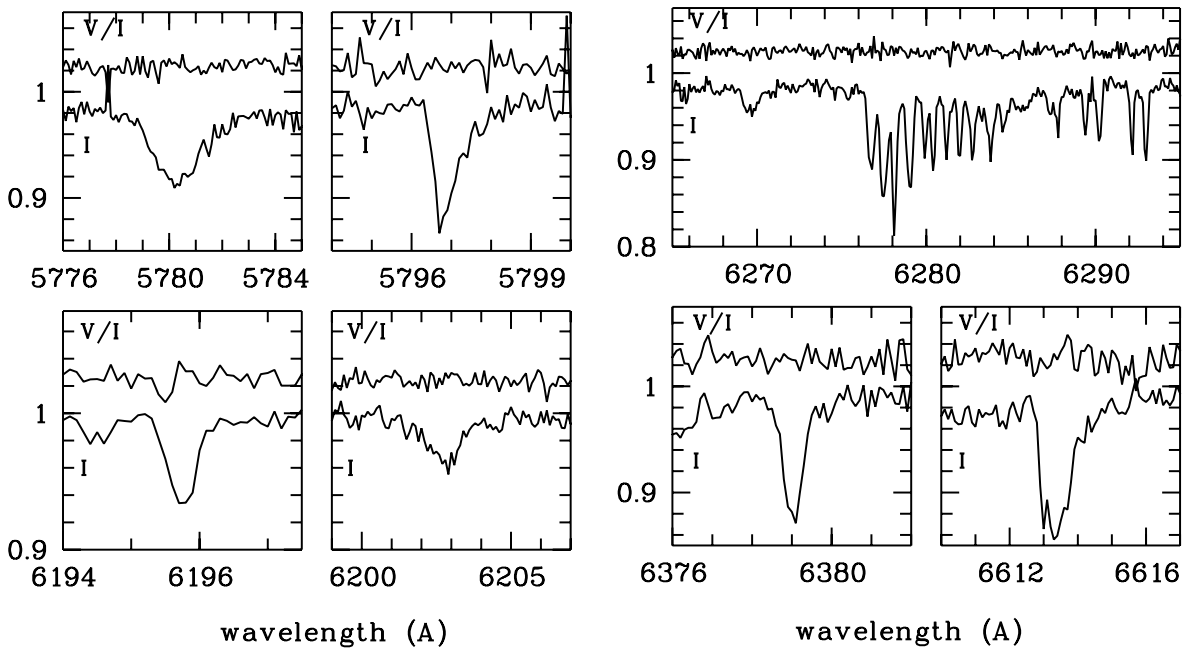

Fig. 6. Circular polarisation: Stokes parameters I and V/I for the 5780, 5797, 6196, 6203, 6284, 6379 and 6613 Å DIBs towards HD 197770. $2\sigma_V$ (per pixel) polarisation noise detection limits are given in Table 4. No significant contamination of stellar lines (for early-type stars) is expected for the DIBs shown above. The B2 III (T = 25 000 K) synthetic spectrum by Gummersbach & Kaufer (1996) shows a 1.5 mÅ Fe II line at 5781.45 Å, a 1.2 mÅ Fe III line at 5796.10 Å and a 22.4 mÅ N II at 6379.62 Å. A few weak (less than 4 mÅ) lines are present in the red wing of the 6284 Å DIB. Several other weak stellar lines in the plotted ranges fall outside the DIB profiles. Note that the atmospheric water lines (the sharp features in the 6284 Å DIB panel) are not polarised.

possible exception of the line of sight towards HD 197770 for which $\eta = 0.001-0.002$ and $f < 0.3$ (Wolff et al. 1997). We find $\eta < 0.01-0.05$ for the studied DIBs towards HD 197770. To further investigate the possible link between the DIBs, the UV bump and the 3.4 μm feature, higher *S/N* polarisation spectra are required.

Thus these findings support the theory that the measured strong DIBs do not directly originate from grains, but rather from gas phase molecules. More stringent detection limits, by at least an order of magnitude, are needed to investigate the extent of this conclusion for weak DIBs and DIBs in the near infrared.

If the DIB carriers are indeed not attached to, or embedded in grains but are gas phase molecules, there are still several mechanisms that could result in the polarisation of absorption profiles, albeit at much smaller levels. And if the transitions responsible for the DIBs are intrinsically polarised, then the DIBs themselves would be either polarised or depolarised relative to the general interstellar polarisation. For instance, one could view PAHs as very small grains (with a diameter less than $\lesssim$30 Å) that as such could give rise to variations in polarisation due to variations of the optical depth similar to what is predicted for the grain related carrier. Obviously, the value of f depends on the properties of the particular carrier molecule. No values for f (or some other equivalent interstellar polarisation efficiency parameter) are currently available for large carbonaceous gas-phase molecules, such as PAHs, but they are expected to be significantly smaller than those inferred for grains.

Linear polarisation is expected for aligned asymmetric molecules or paramagnetic radicals. Polarised light (linear and/or circular) can affect the line intensities of magnetically aligned free molecules (Andrews & Bittner 1991). The orientation or alignment of pendular molecules in the gas phase can also give rise to an optical anisotropy (Slenczka 1999). The eccentricity of aligned small particles, such as PAHs, is a measure of the optical anisotropy, and vice versa (Platt 1956). For larger molecules alignment can be achieved with smaller field strengths due to larger electric dipole moments and smaller rotational constants. PAHs (cations) and fullerenes have non-zero polarizabilities (e.g. Pederson & Quong 1992; Vasvári 1996; Westin et al. 1996). Moreover, the polarisation of electronic transitions (from unbound states) is expected to reveal molecular properties such as the orientation moment in relation to the molecule framework (Dörr 1966).

Several studies show that small graphite particles (like PAHs) cannot be aligned by the Galactic magnetic field in the diffuse ISM (Draine & Malhotra 1993; Draine & Weingartner 1996; Wolff et al. 1997), although possibly suprathermal rotation of PAHs could give rise to a small change in the polarisation signal (Le Coupanec et al. 1998). The (induced) permanent magnetic moment of an ionised dehydrogenated PAH molecule in the diffuse ISM can be as much as 5×10^{-2} μ_B and can be a result of multiple processes: charge rotation, diamagnetism, the Barnett effect, electronic orbital moment and/or spin magnetic moment (Rouan et al. 1992). Harwit (1970) suggested that absorption scattering of starlight is efficient in aligning small grains or large molecules via the intrinsic angular momentum of photons. It is evident that there are still many uncertainties in the physics of the alignment of small grains and large molecules in the diffuse interstellar medium.

Interstellar circular continuum polarisation mechanisms are (e.g. Hough et al. 2001): (i) scattering of linearly polarised radiation off non-Rayleigh particles, which can produce circular polarisation up to an efficiency of 0.5. This could be scattering off aligned grains; (ii) a less efficient mechanism: the combination of several states of linear polarisation produced by birefringent grains (e.g. due to a twist of the magnetic field in a systematic way). In this case, the particles can be grains or molecules.

For an absorption line signal, a circular polarisation of the light (right or left) is produced through the passage of light in a system of chiral molecules (not in the case of a racemic mixture). The asymmetry of the two chiral forms presents itself as an energy difference in the absorption bands. The search for chirality in space is an issue of potential importance to astrobiology. Also, a recent study by Saija et al. (2005) shows that the field inside small cavities in grains is elliptically polarised by incident linear polarised light. This depolarization occurs mainly in the UV, which will give rise to a continuum polarisation due to the interstellar grain size distribution.

No circular line polarisation has been detected towards HD 197770 and HD 163472, with upper limits $2\sigma_V \lesssim 1\%$ and $\lesssim 0.06\%$, respectively. The current lack of understanding of the expected circular line polarisation of chiral gas phase molecules means that this non-detection gives no further insight into the existence of chirality in the Galaxy.

5. Conclusion

In summary, the present results support the hypothesis that DIBs do not originate from grains (or species embedded/attached to grains), but are rather large gas phase molecules, that can survive in the diffuse interstellar medium. The observed DIBs are different in width and in their response to variations in environmental conditions. For example, the 5780 and 6284 Å DIBs are relatively weak (with respect to reddening and the 5797 Å DIB strength) in less UV dominated regions. This is the case for the lines of sight towards HD 197770, while the other sightlines show a relatively stronger 5780 Å DIB. In addition, we studied both DIBs with ($\lambda\lambda$ 5797, 6613) and without ($\lambda\lambda$ 5780, 6284) substructure in the profile, whose carriers are likely of different size, composition and/or structure. This implies that we trace a set of molecules whose effective alignment is affected differently by various molecular properties and interstellar conditions. Our results have therefore covered a broad spectrum of DIB carriers and environments, and represent a strong case for gaseous DIB carriers. New spectropolarimeters, such as ESpaDonS at CFHT, PEPSI at the LBT and NARVAL at the TBL, can establish even more firm upper limits on the polarisation of DIBs and may lead to a detection of the small polarisation signatures expected for aligned PAHs and fullerenes. The possible link between the carriers of the 2175 Å bump, the 3.4 μm diffuse absorption feature and the diffuse interstellar bands (DIBs) warrants also further attention. On the other hand, a quantitative measure of the polarisability/degree of alignment of complex carbonaceous gas phase molecules under conditions prevailing in the diffuse interstellar medium is urgently needed in order to infer information on the physical properties of the DIB carriers.

Acknowledgements. N.L.J.C. was supported by NOVA and PE by VI-NWO (016.023.003). N.C. acknowledges the OPTICON Access program for financial support. We thank the referee for valuable feedback. Our gratitude is also extended toward B. Anthonisse and M. Mokiem for carrying out part of the observational program, and to the TBL staff for their excellent support during the observations.

References

Adamson, A. J., & Whittet, D. C. B. 1992, ApJ, 398, L69
Adamson, A. J., & Whittet, D. C. B. 1995, ApJ, 448, L49
A'Hearn, M. F. 1972, AJ, 77, 302
Andrews, D. L., & Bittner, A. M. 1991, J. Chem. Soc., Faraday Trans., 87, 513
Avery, R. W., Michalsky, J. J., Stokes, R. A., & Ekstrom, P. A. 1975, AJ, 80, 1026
Cami, J., Sonnentrucker, P., Ehrenfreund, P., & Foing, B. H. 1997, A&A, 326, 822
Cami, J., Salama, F., Jiménez-Vicente, J., Galazutdinov, G. A., & Krełowski, J. 2004, ApJ, 611, L113
Chiar, J. E., Adamson, A. J., Whittet, D. C. B., et al. 2006, ApJ, 651, 268
Cox, N. L. J., & Spaans, M. 2006, A&A, 451, 973
Cox, N. L. J., Cordiner, M. A., Cami, J., et al. 2006, A&A, 447, 991
Cox, N. L. J., Cordiner, M. A., Ehrenfreund, P., et al. 2007, A&A, submitted
Crawford, M. K., Tielens, A. G. G. M., & Allamandola, L. J. 1985, ApJ, 293, L45
Donati, J.-F., Semel, M., Carter, B. D., Rees, D. E., & Collier Cameron, A. 1997, MNRAS, 291, 658
Donati, J.-F., Catala, C., Wade, G. A., et al. 1999, A&AS, 134, 149
Dörr, F. 1966, Ang. Chem. Int. Ed. Engl., 5, 478
Draine, B. T., & Malhotra, S. 1993, ApJ, 414, 632
Draine, B. T., & Weingartner, J. C. 1996, ApJ, 470, 551
Ducati, J. R., Ribeiro, D., & Rembold, S. B. 2003, ApJ, 588, 344
Ehrenfreund, P., & Foing, B. H. 1996, A&A, 307, L25
Ehrenfreund, P., Cami, J., Jiménez-Vicente, J., et al. 2002, ApJ, 576, L117
Fahlman, G. G., & Walker, G. A. H. 1975, ApJ, 200, 22
Gammelgaard, P., & Rudkjobing, M. 1973, A&A, 27, 261
Greenberg, J. M., & Hong, S. S. 1974, in Planets, Stars, and Nebulae: Studied with Photopolarimetry, ed. T. Gehrels, IAU Colloq., 23, 916
Gummersbach, C. A., & Kaufer, A. 1996, The Hot Star Newsletter, 22, 16
Harwit, M. 1970, Bull. Astron. Inst. Czech., 21, 204
Heckman, T. M., & Lehnert, M. D. 2000, ApJ, 537, 690
Heger, M. L. 1922, Lick Obs. Bull., 337, 141
Herbig, G. H. 1993, ApJ, 407, 142
Herbig, G. H. 1995, ARA&A, 33, 19
Hough, J. H., Bailey, J. A., Chrysostomou, A., et al. 2001, Adv. Space Res., 27, 313
Jenniskens, P., & Désert, F.-X. 1994, A&AS, 106, 39
Kerr, T. H., Hibbins, R. E., Miles, J. R., et al. 1996, MNRAS, 283, L105
Le Coupanec, P., Rouan, D., & Leger, A. 1998, A&A, 338, 217
Leger, A., & D'Hendecourt, L. 1985, A&A, 146, 81
Martin, P. G., & Angel, J. R. P. 1974, ApJ, 188, 517
Martin, P. G., & Angel, J. R. P. 1975, ApJ, 195, 379
Merrill, P. W. 1934, PASP, 46, 206
Michalsky, J. J., Swedlund, J. B., Stokes, R. A., & Avery, R. W. 1974, ApJ, 187, L13
Neiner, C. 2002, Ph.D. Thesis
Pederson, M. R., & Quong, A. A. 1992, Phys. Rev. B, 46, 13584
Pendleton, Y. J., Sandford, S. A., Allamandola, L. J., Tielens, A. G. G. M., & Sellgren, K. 1994, ApJ, 437, 683
Platt, J. R. 1956, ApJ, 123, 486
Rouan, D., Leger, A., Omont, A., & Giard, M. 1992, A&A, 253, 498
Ruiterkamp, R., Cox, N. L. J., Spaans, M., et al. 2005, A&A, 432, 515
Saija, R., Cecchi-Pestellini, C., Iatì, M. A., et al. 2005, ApJ, 633, 953
Sandford, S. A., Allamandola, L. J., Tielens, A. G. G. M., et al. 1991, ApJ, 371, 607
Sarre, P. J., Miles, J. R., Kerr, T. H., et al. 1995, MNRAS, 277, L41
Serkowski, K., Mathewson, D. L., & Ford, V. L. 1975, ApJ, 196, 261
Slenczka, A. 1999, Chem. – A. Eur. J., 5, 1136
Sollerman, J., Cox, N., Mattila, S., et al. 2005, A&A, 429, 559
Somerville, W. B. 1996, in Polarimetry of the Interstellar Medium, ASP Conf. Ser., 97, 143
Tuairisg, S. Ó., Cami, J., Foing, B. H., Sonnentrucker, P., & Ehrenfreund, P. 2000, A&AS, 142, 225
Valencic, L. A., Clayton, G. C., & Gordon, K. D. 2004, ApJ, 616, 912
Vasvári, B. 1996, Z. Phys. B Cond. Matter, 100, 223
Welty, D. E., Federman, S. R., Gredel, R., Thorburn, J. A., & Lambert, D. L. 2006, ApJS, 165, 138
Westin, E., Rosén, A., Te Velde, G., & Baerends, E. J. 1996, J. Phys. B Atom. Mol. Phys., 29, 5087
Wolff, M. J., Clayton, G. C., Kim, S.-H., Martin, P. G., & Anderson, C. M. 1997, ApJ, 478, 395